

Quantum-like Poincaré-Birkhoff theorem (and some related topics)

F. Borondo

Departamento de Química and
Inst. Mixto de Ciencias Matemáticas CSIC-UAM-UC3M-UCM
Universidad Autónoma de Madrid

Workshop on Instabilities in Hamiltonian Systems
Fields Institute, Toronto, 12-17 June 2011

Abstract

In this talk I will describe some **quantum manifestations** of classical (mainly) chaotic dynamics

Collaborators

- Rosa M. Benito, Universidad Politécnica de Madrid, Spain
- Marcos Saraceno, TANDAR, Comisión Nacional de Energía Atómica, Buenos Aires, Argentina
- D. A. Wisniacki, Universidad de Buenos Aires, Argentina

Outline

- 1 Introduction
 - Aim and Motivation
 - Models
 - Tools
- 2 Invariant tori in quantum mechanics
- 3 Periodic orbits in quantum mechanics: Scars
- 4 Homoclinic and heteroclinic motions
- 5 Quantum-like Poincaré-Birkhoff theorem

Outline

- 1 **Introduction**
 - Aim and Motivation
 - Models
 - Tools
- 2 Invariant tori in quantum mechanics
- 3 Periodic orbits in quantum mechanics: Scars
- 4 Homoclinic and heteroclinic motions
- 5 Quantum-like Poincaré-Birkhoff theorem

Outline

- 1 **Introduction**
 - Aim and Motivation
 - Models
 - Tools
- 2 Invariant tori in quantum mechanics
- 3 Periodic orbits in quantum mechanics: Scars
- 4 Homoclinic and heteroclinic motions
- 5 Quantum-like Poincaré-Birkhoff theorem

Aim

In this respect it should be said that

- **classical chaos** is a well defined phenomenon (i.e. Lyapunov exponent), while
- **quantum chaos** is still a very open question

Motivation

Quantum Mechanics 101

The purpose of this paper is to provide a simple and understandable guide to some of the fundamental ideas of Quantum Mechanics. The reason I'm writing this is because I constantly see that people are being "conned" by people who claim to be experts in Quantum Mechanics, and particularly by the complex and obscure language that these people use. I hope that by imparting a very basic guide to the real concepts behind Quantum Mechanics, more people will be able to see for themselves what's likely to be true or false.

Motivation

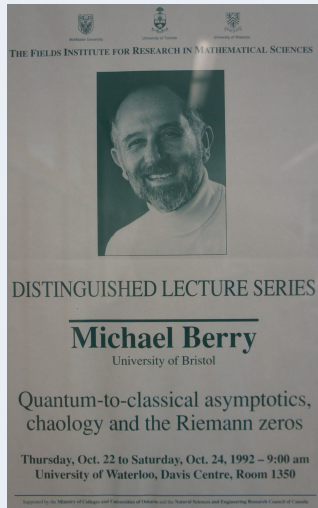
Quantum Cons

This finally leads me on the purpose of this paper. To give the reader some idea of when people are talking sense or not about Quantum Mechanics.

The first “rule” of quantum mechanics is that anything is possible and true, but some things are more probable than others.

The second “rule” of quantum mechanics is that it is impossible to solve anything exactly and prove anything with absolute certainty.

Motivation



Motivation

Physica Scripta. Vol. 40, 335–336, 1989.

Quantum Chaology, Not Quantum Chaos

Michael Berry

H. H. Wills Physics Laboratory, Tyndall Avenue, Bristol BS8 1TL, U.K.

Abstract

There is no quantum chaos, in the sense of exponential sensitivity to initial conditions, but there are several novel quantum phenomena which reflect the presence of classical chaos. The study of these phenomena is quantum chaology.

Motivation

Quantum chaology

Michael Berry

Physics Department, University of Bristol Physics

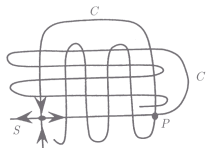
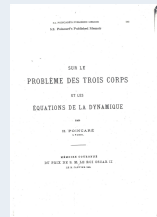
pp104-5 of *Quantum: a guide for the perplexed* by Jim Al-Khalili

(Weidenfeld and Nicolson 2003)

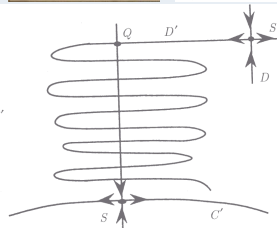
The quantum world appears very different from the world of classical physics that it superseded. Quantum energy levels, wavefunctions and probabilities seem incompatible with Newtonian particles moving along well-defined orbits. Yet the two theories must be intimately related. Even the Moon can be regarded as a quantum particle, so there must be circumstances – roughly, large, heavy objects - where the quantum and classical predictions agree. But the ‘classical limit’ is subtle, and much current research is aimed at understanding it.

Motivation

- In his pioneering work on chaos Poincaré showed the importance of
- Periodic orbits
- Homoclinic solutions
- Heteroclinic solutions



Homoclinic solution



Heteroclinic solution

Motivation

Later (and before), the relevance of other **classical structures** was demonstrated

Today, we will discuss manifestations of

- Invariant tori
- Periodic orbits
- Homoclinic and Heteroclinic motions
- Cantori
- Poincaré-Birkhoff structures

in **Quantum Mechanics**

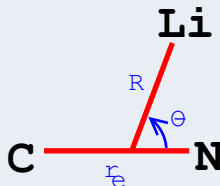
Outline

- 1 **Introduction**
 - Aim and Motivation
 - **Models**
 - Tools
- 2 Invariant tori in quantum mechanics
- 3 Periodic orbits in quantum mechanics: Scars
- 4 Homoclinic and heteroclinic motions
- 5 Quantum-like Poincaré-Birkhoff theorem

LiCN molecule

- Consider molecular vibrations
- From this point of view molecules are
 - collections of oscillators
 - coupled and anharmonic
 - Hamiltonian systems
 - Mixed dynamical phase space

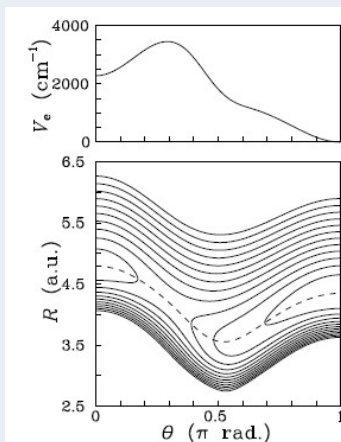
LiCN molecule



$$H = \frac{P_R^2}{2\mu_1} + \frac{1}{2} \left(\frac{1}{\mu_1 R^2} \frac{1}{\mu_2 r_e^2} \right) + V(R, \theta)$$

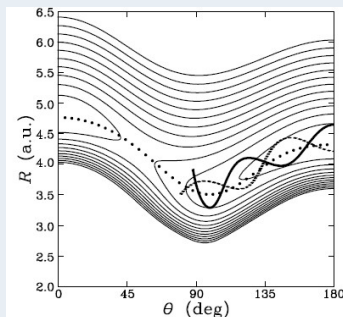
$V(R, \theta)$ is the potential (energy surface)

LiCN molecule



Dotted line: Minimum energy path: $R_e(\theta)$

LiCN molecule



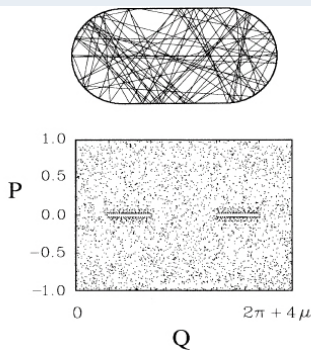
Poincaré surfaces of section:

$$\rho = R - R_e(\theta); \quad \psi = \theta$$

$$P_\rho = P_R; \quad P_\psi = P_\theta + P_R[dR_e/d\theta]$$

Model: Billiards

- Bunimovich stadium billiard
- Hyperbolic dynamics



Model: Quartic oscillator

- $H = \frac{1}{2}(P_x^2 + P_y^2) + \frac{1}{2}x^2y^2 + \frac{\varepsilon}{4}(x^4 + y^4), \quad \varepsilon = 0.01$

- Smooth, homogeneous potential

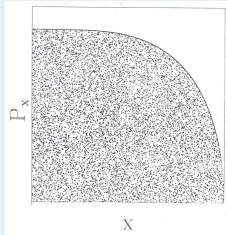
- Mechanical similarity

$$\frac{q}{q_0} = \left(\frac{E}{E_0}\right)^{1/4}, \quad \frac{P}{P_0} = \left(\frac{E}{E_0}\right)^{1/2}, \quad \frac{S}{S_0} = \left(\frac{E}{E_0}\right)^{3/4}, \quad \frac{T}{T_0} = \left(\frac{E}{E_0}\right)^{-1/4}$$

Free from hassles due to phase space evolution (bif's)

SOS: $y = 0, P_y > 0$

- Very chaotic dynamics
- Thought hyperbolic for $\varepsilon \rightarrow 0$
- Dahlqvist and Russberg (1990) found POs for $\varepsilon = 0$
- Also Waterland et al. for $\varepsilon = 1/240$



Model: Quartic oscillator

Carles Simó (forgive me, please)

Model: Harper map

The model that we have chosen to study is the Harper map in the unit square,

$$\begin{aligned}q_{n+1} &= q_n - k \sin(2\pi p_n) \pmod{1}, \\p_{n+1} &= p_n + k \sin(2\pi q_n) \pmod{1},\end{aligned}\tag{1}$$

where k is a parameter measuring the strength of the perturbation. This map can be understood as the stroboscopic version of the flow corresponding to the (kicked) Hamiltonian

$$H(p, q, t) = -\frac{1}{2\pi} \cos(2\pi p) - \frac{k}{2\pi} \cos(2\pi q) \sum_n \delta(t - nk).\tag{2}$$

Outline

- 1 Introduction
 - Aim and Motivation
 - Models
 - Tools
- 2 Invariant tori in quantum mechanics
- 3 Periodic orbits in quantum mechanics: Scars
- 4 Homoclinic and heteroclinic motions
- 5 Quantum-like Poincaré-Birkhoff theorem

Phase space representations of QM

- Wigner transform (1932)

JUNE 1, 1932

PHYSICAL REVIEW

VOLUME 40

On the Quantum Correction For Thermodynamic Equilibrium

By E. WIGNER

Department of Physics, Princeton University

(Received March 14, 1932)

The probability of a configuration is given in classical theory by the Boltzmann formula $\exp \{-V/kT\}$ where V is the potential energy of this configuration. For high temperatures this of course also holds in quantum theory. For lower temperatures, however, a correction term has to be introduced, which can be developed into a power series of \hbar . The formula is developed for this correction by means of a probability function and the result discussed.

$$W(q, P) = \int ds \, e^{isP} \psi^* \left(q - \frac{s}{2} \right) \psi \left(q + \frac{s}{2} \right)$$

But ...

- $W(q, P)$ can be negative

- **Why?:**

Heisenberg's uncertainty principle

- Solution: **Husimi function**

- Gaussian average in cells of area \hbar^N

$$H(q, P) = \int \int_{\hbar^N} dq' dP' G_{q, P}(q', P') W(q', P')$$

- Coherent state representation

$$H(q, P) = \frac{1}{(2\pi\hbar)^N} |\langle \phi_{q, P} | \psi \rangle|^2$$

ϕ minimum uncertainty coherent state

$$\phi(x, y, P_x, P_y) = \left[\frac{2\alpha}{\pi} \right]^{1/4} e^{-\alpha(x-x_0)^2} e^{-\alpha(y-y_0)^2} e^{iP_x^0 x} e^{iP_y^0 y}$$

But ...

- $W(q, P)$ can be negative
- **Why?:**
Heisenberg's uncertainty principle
- Solution: **Husimi function**

- Gaussian average in cells of area \hbar^N

$$H(q, P) = \int \int_{\hbar^N} dq' dP' G_{q, P}(q', P') W(q', P')$$

- Coherent state representation

$$H(q, P) = \frac{1}{(2\pi\hbar)^N} |\langle \phi_{q, P} | \psi \rangle|^2$$

ϕ minimum uncertainty coherent state

$$\phi(x, y, P_x, P_y) = \left[\frac{2\alpha}{\pi} \right]^{1/4} e^{-\alpha(x-x_0)^2} e^{-\alpha(y-y_0)^2} e^{iP_x^0 x} e^{iP_y^0 y}$$

But ...

- $W(q, P)$ can be negative
- **Why?:**
Heisenberg's uncertainty principle
- Solution: **Husimi function**

- Gaussian average in cells of area \hbar^N

$$H(q, P) = \int \int_{\hbar^N} dq' dP' G_{q,P}(q', P') W(q', P')$$

- Coherent state representation

$$H(q, P) = \frac{1}{(2\pi\hbar)^N} |\langle \phi_{q,P} | \psi \rangle|^2$$

ϕ minimum uncertainty coherent state

$$\phi(x, y, P_x, P_y) = \left[\frac{2\alpha}{\pi} \right]^{1/4} e^{-\alpha(x-x_0)^2} e^{-\alpha(y-y_0)^2} e^{iP_x^0 x} e^{iP_y^0 y}$$

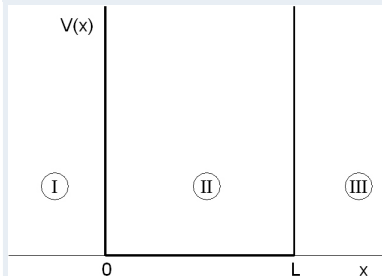
Zeros of the Husimi function

- **Maxima** of the Husimi function appear localized on the important parts of the quantum density
- Leboeuf and Voros showed that the **zeros** give also relevant information
 - Regular states: they appear on a line, sitting at the **nodes**
 - Irregular/chaotic states: they spread over all available phase space

Outline

- 1 Introduction
 - Aim and Motivation
 - Models
 - Tools
- 2 Invariant tori in quantum mechanics
- 3 Periodic orbits in quantum mechanics: Scars
- 4 Homoclinic and heteroclinic motions
- 5 Quantum-like Poincaré-Birkhoff theorem

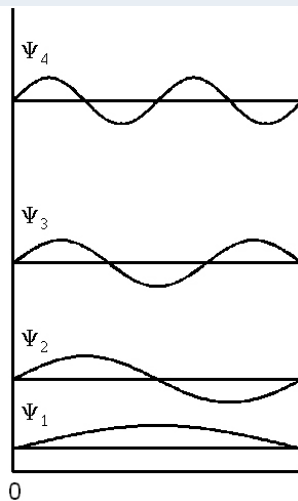
Simpler example (even trivial), QM101



- $\psi_I = \psi_{III} = 0$
- $-\frac{\hbar^2}{2m} \frac{d^2 \psi_{II}}{dx^2} + V \psi_{II} = E \psi_{II}$
- $\frac{d^2 \psi_{II}}{dx^2} + k^2 \psi_{II}, \quad k = \frac{\sqrt{2mE}}{\hbar}$
- But, **don't forget** the dynamics:
 $k = \frac{p}{\hbar}$

Solution

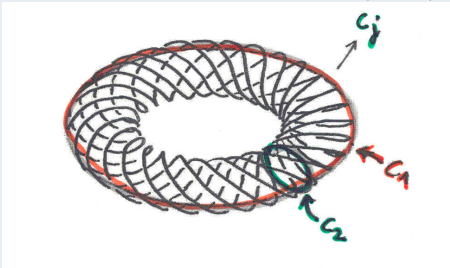
- $\psi(x) = a \sin kx + b \cos kx$
- First boundary condition:
 $\psi(0) = 0 \rightarrow b = 0$
 $\psi = a \sin kx$
- Normalization condition:
 $\int_0^L |\psi|^2 dx = 1 \rightarrow a = \sqrt{\frac{2}{L}}$
- Second boundary condition:
 $\psi(L) = 0 \rightarrow k_n = \frac{n\pi}{L}$
- Solutions: $\psi_n(x) = \sqrt{\frac{2}{L}} \sin \frac{n\pi x}{L}, \quad n = 1, 2, \dots$



- But, **don't forget** the dynamics . . . $k = \frac{P}{\hbar}$
- Classical action:
$$\oint P dx = 2 \int_0^L P dx = 2 \int_0^L k \hbar dx = 2k \hbar L = 2 \frac{n\pi}{L} \hbar L = nh$$
- **Action is quantized in QM!**
- Classical actions \equiv Quantum numbers

Quantization of the action. How?

- Einstein–Brillouin–Kramers (EBK) Method



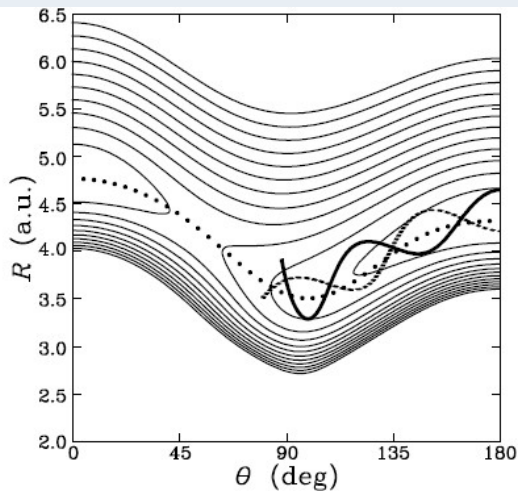
$$\oint_{C_j} \sum_i^N P_i dq_i = h \left(n_j + \frac{\alpha_j}{4} \right)$$

Classical info = Quantum condition

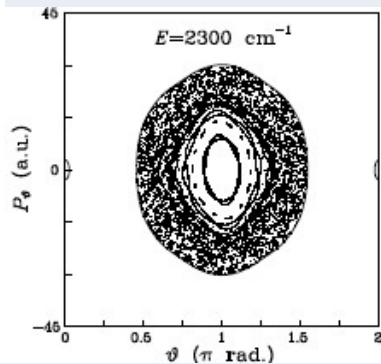
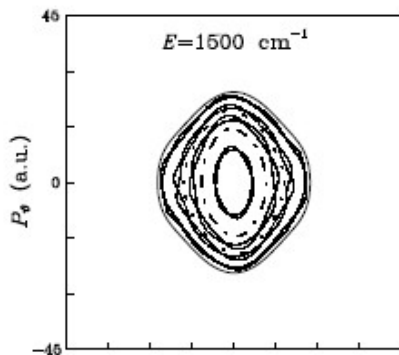
- Associated WKB (Wentzel–Kramers–Brillouin) wave function

$$\psi(q) = \sum_j A_j e^{iS_j(q)/\hbar}$$

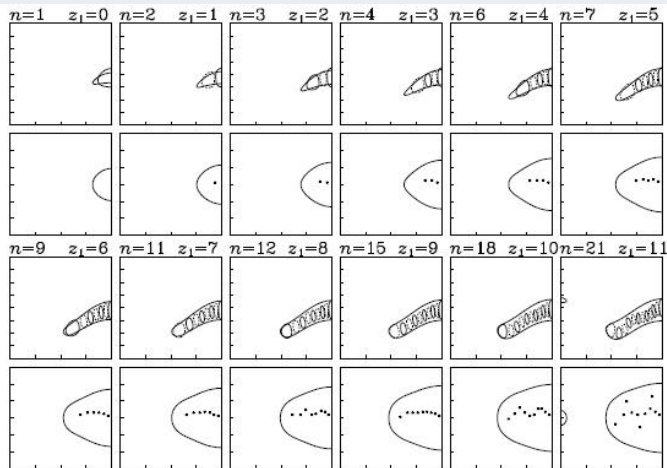
Example: LiCN



Example: LiCN



Example: LiCN



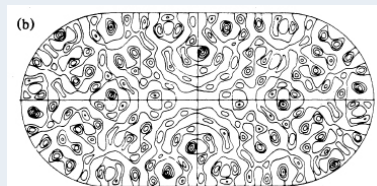
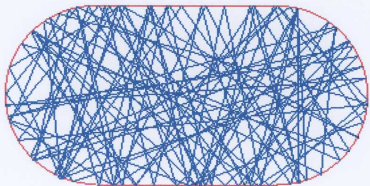
Outline

- 1 Introduction
 - Aim and Motivation
 - Models
 - Tools
- 2 Invariant tori in quantum mechanics
- 3 Periodic orbits in quantum mechanics: Scars
- 4 Homoclinic and heteroclinic motions
- 5 Quantum-like Poincaré-Birkhoff theorem

Periodic orbits in quantum mechanics: Scars

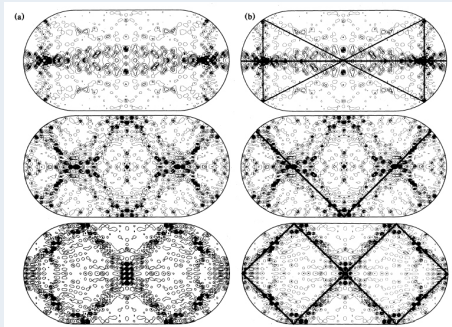
- What are scars?

Expected: Chaotic classical dynamics \longrightarrow uniformly distributed quantum density



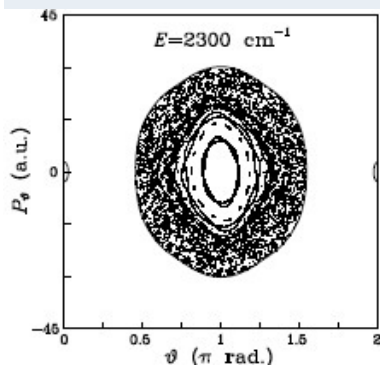
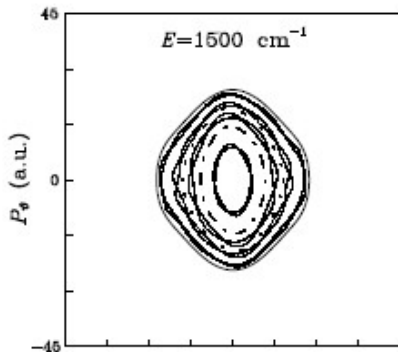
Scarred functions

- But in numerical calculations ...



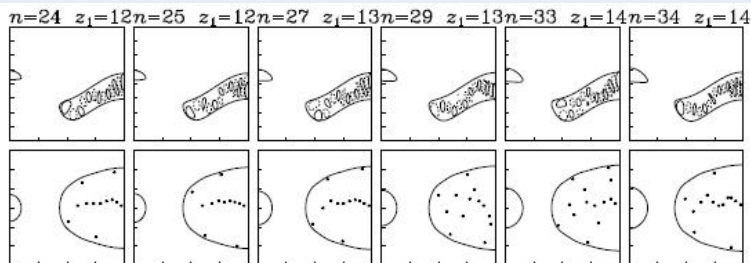
Heller in 1984 coined the term **scar** to name an enhanced localization of quantum probability density of certain eigenstates on classical unstable **periodic orbits**

Scars and the zeros of the Husimi function



Husimi zeroes also tell about scarred states!

Scars and the zeros of the Husimi function



Husimi zeroes also tell about scarred states!

Scars still generate interest after 25 years

Scars in Optical Fibers

VOLUME 88, NUMBER 1

PHYSICAL REVIEW LETTERS

7 JANUARY 2002

Light Scarring in an Optical Fiber

Valérie Doya, Olivier Legrand, and Fabrice Mortessagne

Laboratoire de Physique de la Matière Condensée, CNRS UMR 6622, Université de Nice Sophia-Antipolis, 06108 Nice, France

Christian Miniatura

Laboratoire Ondes et Désordre, CNRS FRE 2302, 1361 route des Lucioles, Sophia-Antipolis, F-06560 Valbonne, France

(Received 31 July 2001; published 18 December 2001)

We report the first experimental study of wave scarring in an optical fiber with a noncircular cross section. This optical multimode fiber serves as a powerful tool to image waves in a system where light rays exhibit a chaotic dynamics. Far-field intensity measurements are used to provide a better identification of scars in the Fourier domain. This first experimental characterization of scarring effect in optics demonstrates the relevance of such an optical waveguide for novel experiments in wave chaos.

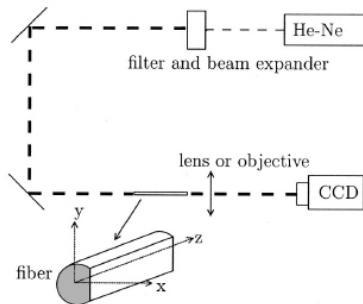
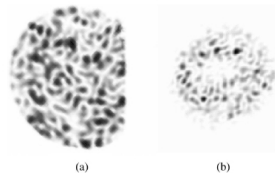
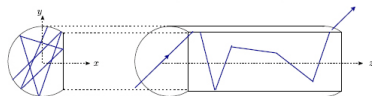
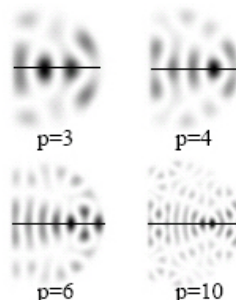


FIG. 14. Experimental setup.

FIG. 1. Typical specklelike experimental intensity pattern at the output of a chaotic D-shaped fiber for a plane wave illumination at central wave vector $\kappa_c = 19.0R^{-1}$. (a) Near-field intensity; (b) far-field intensity.

Scars in Microcavity lasers

VOLUME 88, NUMBER 9

PHYSICAL REVIEW LETTERS

4 MARCH 2002

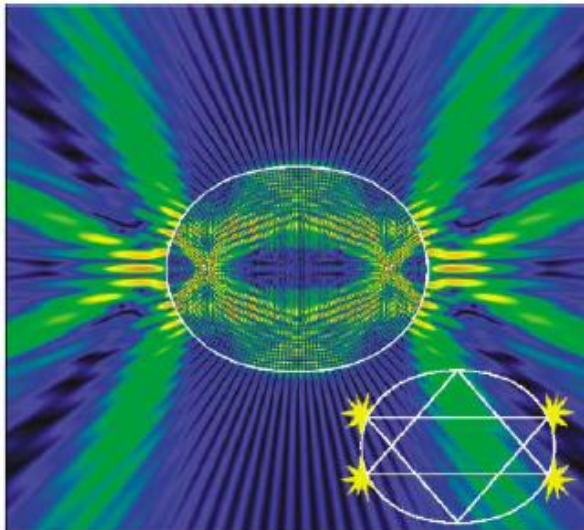
Fresnel Filtering in Lasing Emission from Scarred Modes of Wave-Chaotic Optical Resonators

N. B. Rex, H. E. Tureci, H. G. L. Schwefel, R. K. Chang, and A. Douglas Stone

Department of Applied Physics, P.O. Box 208284, Yale University, New Haven, Connecticut 06520-8284

(Received 24 May 2001; published 19 February 2002)

We study lasing emission from asymmetric resonant cavity GaN microlasers. By comparing far-field intensity patterns with images of the microlaser we find that the **lasing modes are concentrated on three-bounce unstable periodic ray orbits; i.e., the modes are scarred.** The high-intensity emission directions of these scarred modes are completely different from those predicted by applying Snell's law to the ray orbit. This effect is due to the process of "Fresnel filtering" which occurs when a beam of finite angular spread is incident at the critical angle for total internal reflection.



(Relativistic) Scars in Graphene sheets

PRL 103, 054101 (2009)

PHYSICAL REVIEW LETTERS

week ending
31 JULY 2009



Relativistic Quantum Scars

Liang Huang,¹ Ying-Cheng Lai,^{1,2} David K. Ferry,^{1,2,3} Stephen M. Goodnick,^{1,2,3} and Richard Akis^{1,3}

¹*Department of Electrical Engineering, Arizona State University, Tempe, Arizona 85287, USA*

²*Department of Physics, Arizona State University, Tempe, Arizona 85287, USA*

³*Center for Solid State Electronics Research, Arizona State University, Tempe, Arizona 85287, USA*

(Received 27 February 2009; published 27 July 2009)

The concentrations of wave functions about classical periodic orbits, or quantum scars, are a fundamental phenomenon in physics. An open question is whether scarring can occur in relativistic quantum systems. To address this question, we investigate confinements made of graphene whose classical dynamics are chaotic and find unequivocal evidence of relativistic quantum scars. The scarred states can lead to strong conductance fluctuations in the corresponding open quantum dots via the mechanism of resonant transmission.

(Relativistic) Scars in Graphene sheets

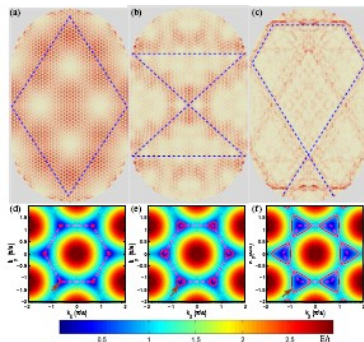


FIG. 1 (color online). Typical quantum scars [red (darker region) indicates higher electron concentration] for a stadium-shaped graphene confinement with zigzag horizontal boundaries and contour plots of energy in the wave vector plane (the band structure). The energies for the patterns in (a-c) are $E/t = 0.13252, 0.4024, \text{ and } 0.91188$, respectively. The stadium consists of $N = 11814$ carbon atoms. Panels (d-f) show the $E - k$ configuration for an infinite graphene flake for the same lattice orientation and energy values as those for (a-c), respectively. The allowed wave vectors are on the constant energy curves (as indicated by the arrows). The lattice constant is $a = 2.46 \text{ \AA}$. Dashed line segments in (a-c) are for eye guidance, and in (d-f) they indicate the first Brillouin zone.

(Relativistic) Scars in Graphene sheets

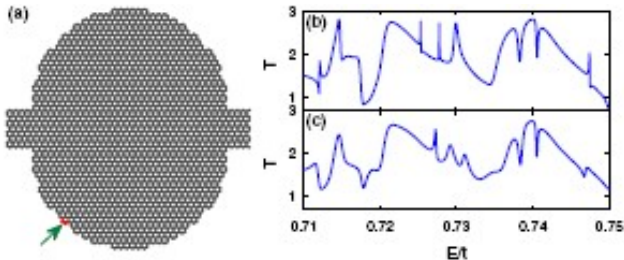


FIG. 4 (color online). (a) An open stadium-shaped graphene quantum dot with semi-infinite leads on both sides. The shape has a mirror symmetry. (b) Transmission T versus energy E/t . (c) Transmission T for the dot after removing the two carbon atoms as indicated by the arrow in (a) so that the mirror symmetry is broken.

(Relativistic) Scars in Graphene sheets

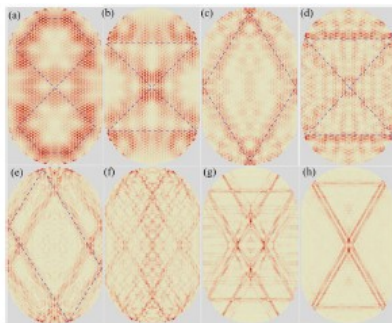


FIG. 2 (color online). Typical scars in the stadium-shaped graphene confinement as in Fig. 1. The energy values for (a–h) are $E/t = 0.25347, 0.36358, 0.57665, 0.60699, 0.81956, 0.91061, 0.97722, \text{ and } 0.99198$, respectively. The dashed lines represent classical periodic orbits.

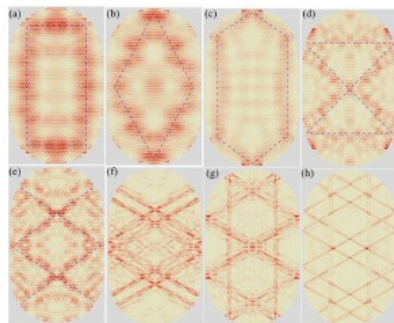
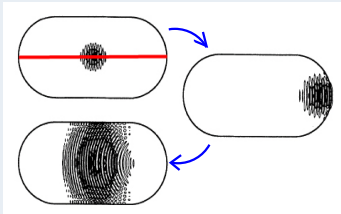


FIG. 3 (color online). Scars in stadium-shaped graphene confinement with armchair horizontal boundaries. The number of atoms is $N = 13694$. The corresponding energy values are $E/t = 0.20031, 0.2599, 0.3106, 0.54954, 0.59238, 0.9168, 0.95216, \text{ and } 0.99801$ for (a–h), respectively.

Why do scars happen?

Heller's dynamical explanation for scars



Recurrences

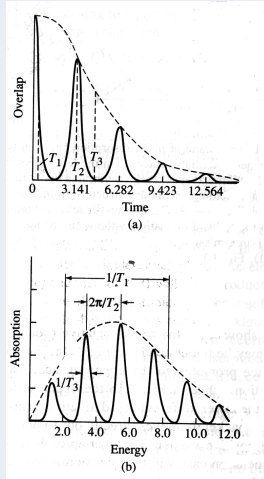
Fourier transform
between:

correlation function

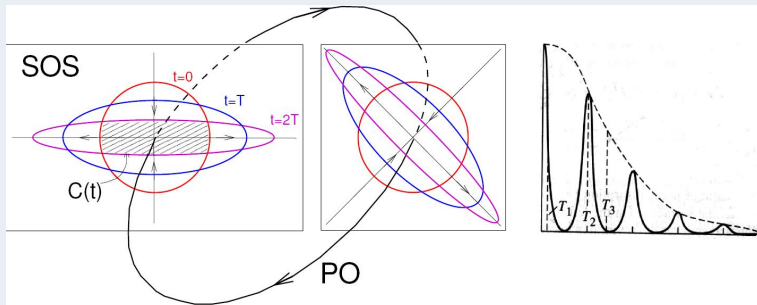
$C(t) = \langle \phi(0) | \phi(t) \rangle$, and

corresponding **spectrum**

$$I(E) = \int dt e^{iEt/\hbar} C(t)$$



Recurrences



Peaks

- **Where?**

Bohr–Sommerfeld quantization condition on the action:

$$S = \oint P \cdot dq = 2\pi\hbar \left(n + \frac{\alpha}{4}\right)$$

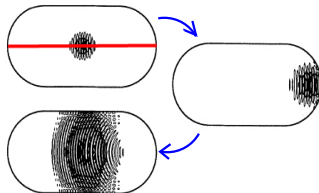
- **Why?**

Constructive interference in the WKB wavefunction

$$\psi(q) = A e^{iS(q)/\hbar}$$

BUT ...

What happens to the density that does not come back in the recurrence along the scarring periodic orbit?

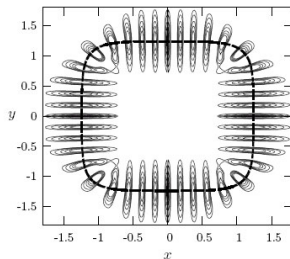


This is the question that will be addressed now

How to systematically construct scar functions

- Borondo et al., PRL 73, 1613 (1994); **version 2007**
- Wavepacket initially localized on the PO

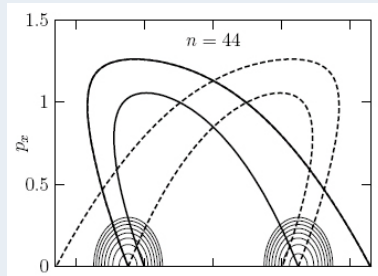
$$\psi_{\text{tube}}(x, y) = N \int_0^T dt e^{-\alpha_x(x-x_t)^2 - \alpha_y(y-y_t)^2} \times \cos \left[S_t - \frac{\mu\pi t}{2T} + P_{xt}(x - x_t) + P_{yt}(y - y_t) \right]$$



In phase space

- Quantum SOS based on Husimi function:

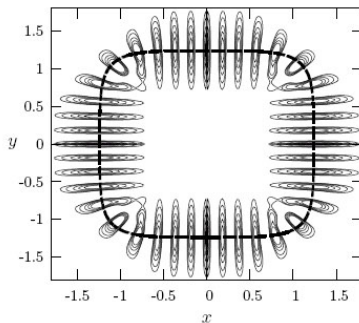
$$\mathcal{H}(x, P_x) = \left| \int_{-\infty}^{\infty} dx' e^{-(x-x')^2/(2\alpha_H^2) - iP_x x'} \psi(x', y' = 0) \right|^2$$



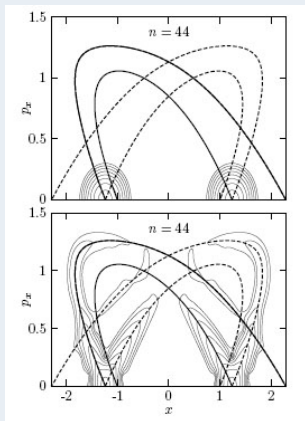
This can be improved

- Propagate $\psi_{\text{tube}}(x, y)$ in time and Fourier transform at E_{BS}

$$\psi_{\text{scar}}(x, y) = N \int_{-T_E}^{T_E} dt \cos\left(\frac{\pi t}{2T_E}\right) e^{-i(\hat{H}-E_{\text{BS}})t} \psi_{\text{tube}}(x, y)$$



Same in phase space

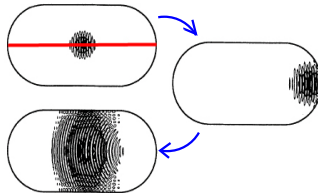


$$\psi_{\text{tube}}(x, y)$$

$$\psi_{\text{scar}}(x, y)$$

Lets us return to our previous question:

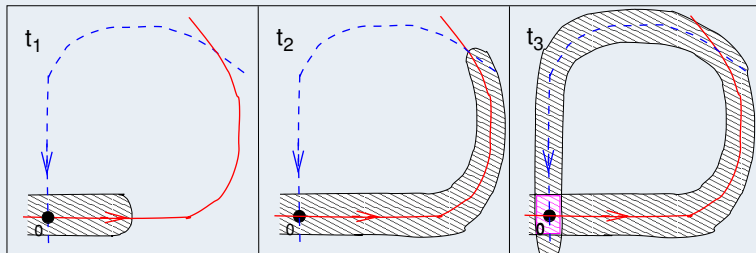
What happens to the density that does not come back in the recurrence along the scarring periodic orbit?



Outline

- 1 Introduction
 - Aim and Motivation
 - Models
 - Tools
- 2 Invariant tori in quantum mechanics
- 3 Periodic orbits in quantum mechanics: Scars
- 4 **Homoclinic and heteroclinic motions**
- 5 Quantum-like Poincaré-Birkhoff theorem

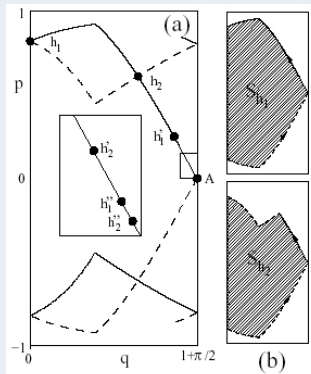
The rest will leave the PO along the unstable manifold, and the main part will return using two homoclinic circuits.



Homoclinic motion and eigenvalues

Phys. Rev. Lett. 94, 054101 (2005)

The rest will leave the PO along the unstable manifold, and the main part will return using two homoclinic circuits.



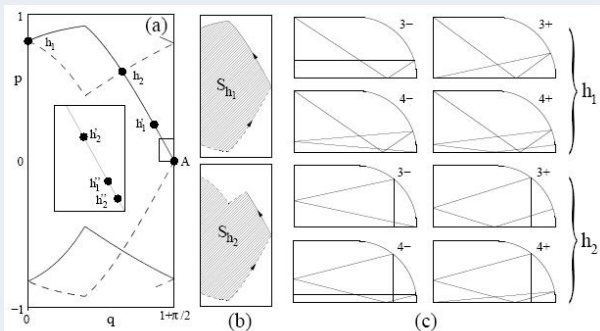
Quantization of the homoclinic torus

Under which circumstances the homoclinic trajectory **reinforce** the **quantization** of the central one?

- Quantization horizontal PO: $kL_H - \frac{\pi}{2}\nu_H = 2\pi n_H$
Scar condition
- Quantization homoclinic torus: $kL_{HT} - \frac{\pi}{2}\nu_{HT} = 2\pi n_{HT}$
- These two conditions can be combined into a single one:
 $k(L_{HT} - L_H) - \frac{\pi}{2}(\nu_{HT} - \nu_H) = 2\pi(n_{HT} - n_H)$

Quantizing the homoclinic torus

- The homoclinic motions (both h_1 and h_2) can be approximated by two families of satellite PO's (Ozorio de Almeida)

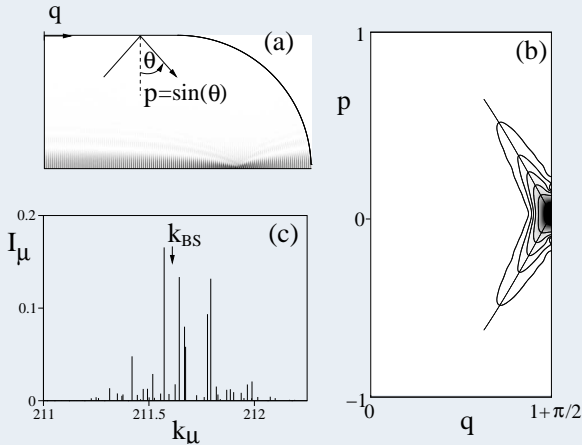


- Quantization horizontal PO: $kL_H - \frac{\pi}{2}\nu_H = 2\pi n_H$
- Quantization m -th satellite PO: $kL_m - \frac{\pi}{2}\nu_m = 2\pi n_m$
- Combination
 $k(L_m - mL_H) - \frac{\pi}{2}(\nu_m - m\nu_H) = 2\pi(n_m - mn_H)$

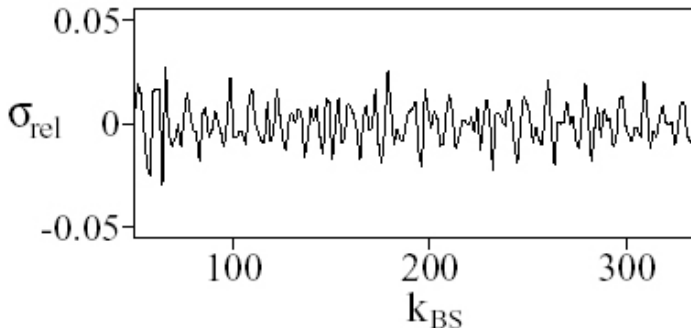
m	$\overline{L}_m - mL_H$	
	Family h ₁	Family h ₂
3	-3.367 727 48	-2.990 915 39
4	-3.368 367 57	-2.991 131 87
5	-3.368 389 68	-2.991 141 81
6	-3.368 390 43	-2.991 142 21
7	-3.368 390 45	-2.991 142 22

- Which should be the effect in QM – Scarred states?
- When both quantization conditions are fulfilled the scarred state is better defined
- When only the PO is quantized the scarred state is worse defined
- Then, when projecting the scars on the spectrum the width should fluctuate periodically with the excitation number along the PO

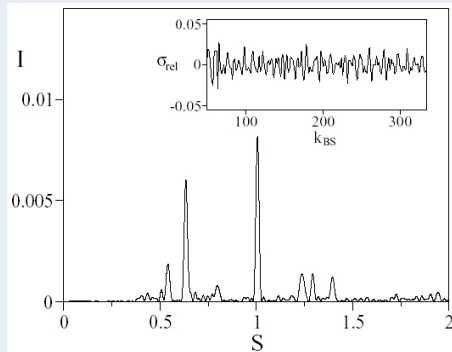
- Project **scar functions** on eigenstates spectrum



- Compute $\sigma = \sqrt{\sum_n |\langle n|\psi\rangle|^2 (k_n^2 - k_{BS}^2)}$
- Scale σ and make them adimensional
 $\sigma_{rel} = \frac{\sigma - \sigma_{sc}}{\sigma_{sc}}; \quad \sigma_{sc} = \frac{\pi \hbar \lambda}{|\ln \hbar|}; \quad \lambda \text{ Lyapunov exp}$

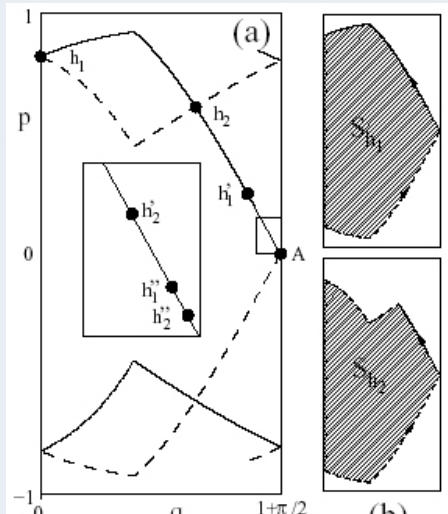


- Now Fourier analyze the signal
"The noise is the signal" (Landauer)



- Peaks at $S = 0.633$ and 1.007
Also at $S = -3.367$ and -2.993 , since FT is $L_H = 4$ periodic

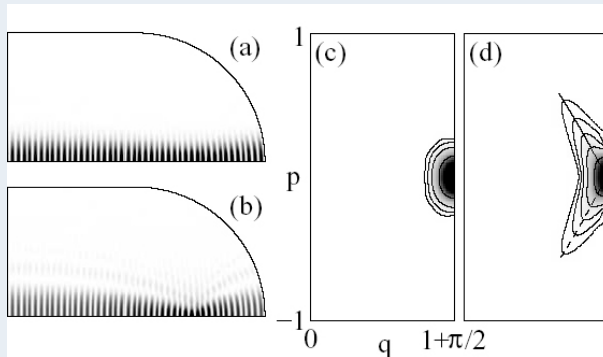
- Peaks coincide with the value of primary **homoclinic areas**



Homoclinic motion and wave functions

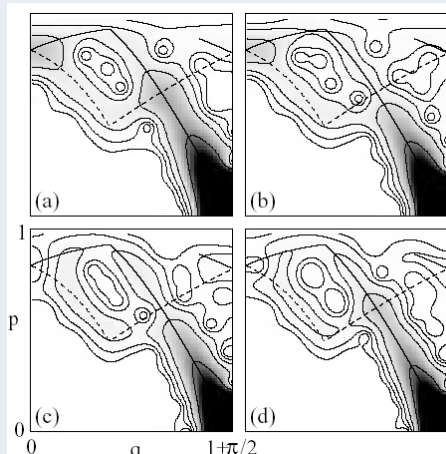
Phys. Rev. Lett. 97, 094101 (2006)

$$\bullet \quad |\phi_{\text{scar}}\rangle = \int_{-T}^T dt \cos\left(\frac{\pi t}{2T}\right) e^{i(E_{\text{BS}} - \hat{H})t/\hbar} |\phi_{\text{tube}}\rangle$$

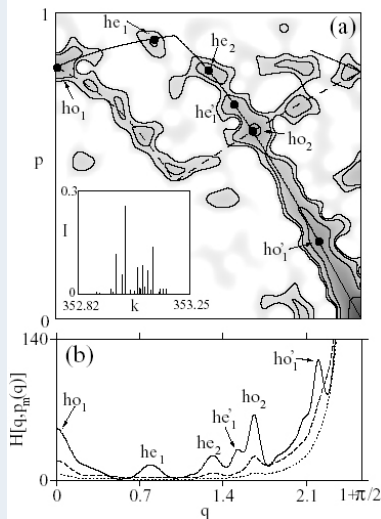


Husimidis for 4 scar function with quantization/antiquantization conditions on the homoclinic torus (all quantized on the PO)

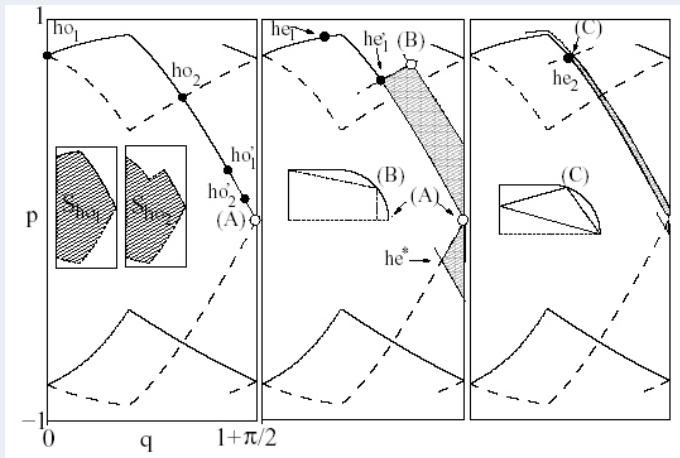
Label	n_H	k_{BS}	n_{ho1}	n_{ho2}
(a)	34	54.585	29.01	25.99
(b)	40	64.010	34.07	30.47
(c)	44	70.293	37.43	33.46
(d)	50	79.718	42.49	37.95



- Scar function $n = 224$
- Homoclinic quantization:
 $n_{h_1} = 189.01, n_{h_2} = 168.07$
- Extra quantization on heteroclinic orbits:
 $kS_{he} = 2\pi n_{he}$
 $n_{he_1} = 19.00, n_{he_2} = 5.98$
- Husimis for $T = 0.9t_E, 1.2t_E$
 and $3.3t_E$



Classical phase space



Unveiling other classical invariants

Even other classical invariants can be unveiled in QM
i.e. Lazutkin homoclinic invariant
(thanks to Enerst Fontich)

EPL, 89 (2010) 40013
doi: 10.1209/0295-5075/89/40013

www.epljournal.org

Diagonal matrix elements in a scar function basis set

E. G. VERGINI^{1,2(a)}, E. L. SIBERT III³, F. REVUELTA², R. M. BENITO² and F. BORONDO⁴

Abstract – We provide canonically invariant expressions to evaluate diagonal matrix elements of powers of the Hamiltonian in a scar function basis set. As a function of the energy, each matrix element consists of a smooth contribution associated with the central periodic orbit, plus oscillatory contributions given by a finite set of relevant homoclinic orbits. Each homoclinic contribution depends, in leading order, on four canonical invariants of the corresponding homoclinic orbit; a geometrical interpretation of these not well-known invariants is given. The obtained expressions are verified in a chaotic coupled quartic oscillator.

GELFREICH V. G., LAZUTKIN V. F. and SVANIDZE N. V.,
Physica D, 71 (1994) 82.

Cantori in QM

VOLUME 57, NUMBER 23

PHYSICAL REVIEW LETTERS

8 DECEMBER 1986

Kolmogorov-Arnol'd-Moser Barriers in the Quantum Dynamics of Chaotic Systems

T. Geisel, G. Radons, and J. Rubner

Institut für Theoretische Physik, Universität Regensburg, D-8400 Regensburg, West Germany

(Received 18 August 1986)

Classical Kolmogorov-Arnol'd-Moser tori and cantori are found to act as barriers in the quantum dynamics of a kicked rotator. In their vicinity the asymptotic distribution decays exponentially. The penetration depth of a Kolmogorov-Arnol'd-Moser torus scales as $\hbar^{0.66}$ and the penetration probability as $\hbar^{2.5}$. Cantori can inhibit the diffusive growth of mean square displacements and thus act as barriers more drastically than in classical systems.

Cantori in QM

Barriers to Chaotic Classical Motion and Quantum Mechanical Localization in Multiphoton Dissociation

Robert C. Brown[†] and Robert E. Wyatt^{*}

*Institute of Theoretical Chemistry and Department of Chemistry, University of Texas,
Austin, Texas 78712-1167 (Received: January 15, 1986)*

Recent work (MacKay, R. S.; Meiss, J. D.; Percival, I. C. *Physica D* **1984**, *13*, 55. Bensimon, D.; Kadanoff, L. E. *Physica D* **1984**, *13*, 82.) on locating and calculating the flux across global bottlenecks to classical diffusion in strongly chaotic regions is used to study IR multiphoton dissociation for a model diatomic molecule. Particular attention is given to the correspondence between the classical barriers and quantum mechanical dissociation rates. It is found that quantum mechanical localization can arise in regions of x - p phase space which are strongly stochastic when the classical flux is smaller than \hbar .

Cantori in QM

The classical Hamiltonian for a nonrotating diatomic interacting with a laser field can be written²²

$$H_C = H_M + H_F + \lambda H_I = E \quad (1)$$

where H_F and H_M are Hamiltonians for the radiation field and the HF (Morse oscillator) diatomic, respectively, and H_I is the field-molecule, nonlinear, dipole interaction

$$H_M = p^2/(2\mu) + D_0[1 - e^{-\alpha(x-x_0)}]^2 \quad (2a)$$

$$H_F = (1/2)[P_F^2 + \omega_F^2 X_F^2] \quad (2b)$$

$$H_I = -D(x)X_F \quad (2c)$$

with

$$D(x) = Ax \exp\{-\beta x^4\} \quad (2d)$$

The coupling parameter is related to the radiation field strength E_0 and intensity I by

$$\lambda = \omega_F E_0 / (2E)^{1/2} = \omega_F [I / c \epsilon_0]^{1/2} \quad (3)$$

where c is the speed of light, ϵ_0 is the permittivity of free space, and E is the conserved total energy of the laser/oscillator system

Cantori in QM

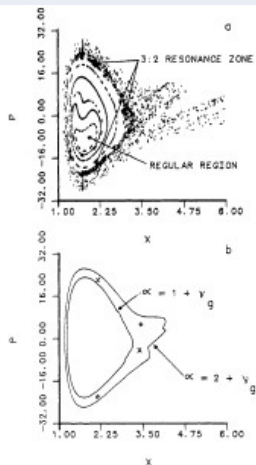


Figure 1. The x - p surface of section for the Hamiltonian describing the interaction between an anharmonic oscillator and an intense radiation field. (b) Phase space representation of the cantori resulting from the breakup of KAM surfaces with winding numbers equal to 1 and 2 plus the golden mean. Also shown are the fixed points for a stable (O) and

Cantori in QM

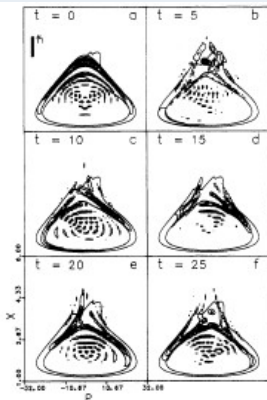


Figure 5. Cantori plots (positive contours only) for the Wigner transform of a nonstationary state for an anharmonic oscillator evolving in response to the radiation field after (a) 0, (b) 5, (c) 10, (d) 15, (e) 20, and (f) 25 field periods ($1\tau = 0.054$ ps). The cantori shown in Figure 1b are also shown in each of the diagrams a-f. The oscillator was initially, Figure 5a, in the 15-th Morse eigenstate.

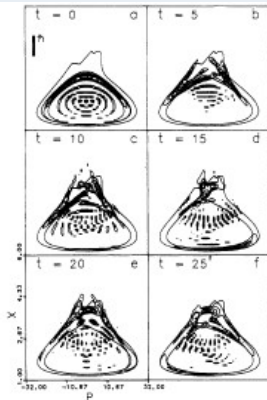


Figure 6. Same as Figure 5, except the diatomic was initially, Figure 6a, in the 13-th Morse eigenstate.

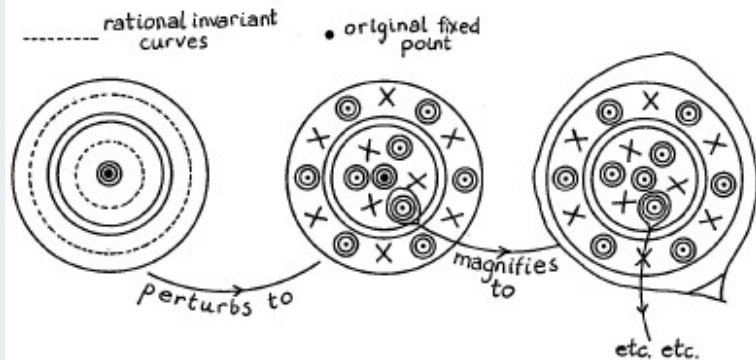
up under the nonlinear coupling. Other oscillator states which initially lie between the cantori (e.g., the 12-th and 14-th) show a similar behavior. However, since these states are not resonantly

Outline

- 1 Introduction
 - Aim and Motivation
 - Models
 - Tools
- 2 Invariant tori in quantum mechanics
- 3 Periodic orbits in quantum mechanics: Scars
- 4 Homoclinic and heteroclinic motions
- 5 Quantum-like Poincaré-Birkhoff theorem

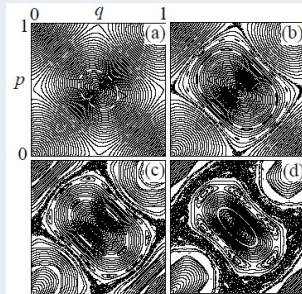
Classical Poincaré-Birkhoff theorem

After Berry.



Harper map: classical dynamics

$$\begin{aligned}q_{n+1} &= q_n - k \sin(2\pi p_n) \pmod{1}, \\p_{n+1} &= p_n + k \sin(2\pi q_n) \pmod{1},\end{aligned}\tag{3}$$



for k : (a) 0.1, (b) 0.155, (c) 0.2, and (d) 0.25.

Harper map: quantum dynamics

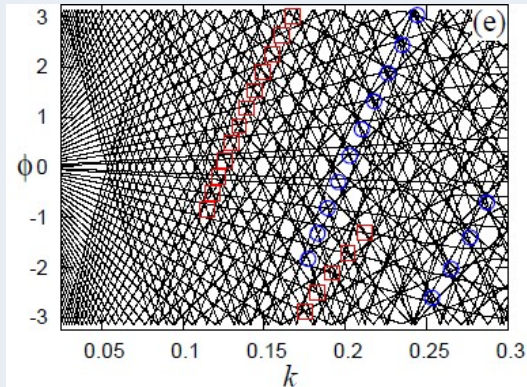
The idea is to construct and diagonalize an *evolution operator*

$$\hat{U} = e^{-i\hat{H}T/\hbar} = \exp[iNk \cos(2\pi\hat{q})] \exp[iNk \cos(2\pi\hat{p})],$$
$$N = (2\pi\hbar)^{-1}$$

The simplicity of this model allows extremely detailed calculations.

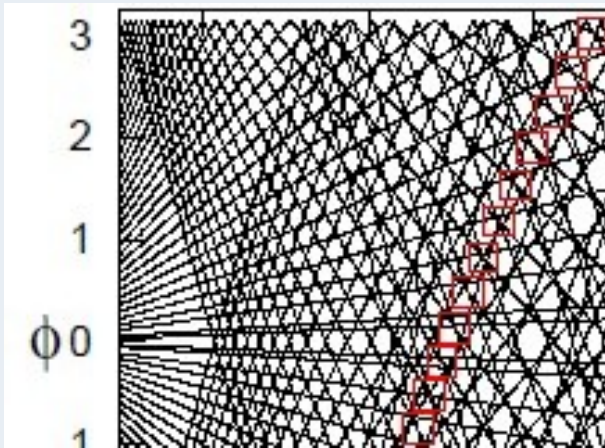
Diagonalization gives a series of eigenphases: $\phi_n = e^{iE_n T}$

Eigenphases correlation diagram



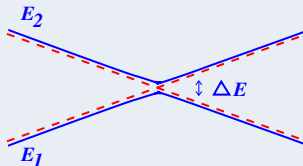
$\Delta n = 10$ (red squares); $\Delta n = 6$ (blue circles)

Eigenphases correlation diagram

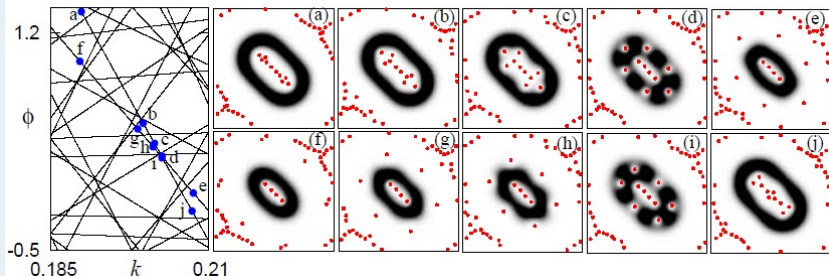


Avoided crossings

- States avoid crossing due to the Wigner-von Neumann rule
- Locally states interact by pairs: $\{\psi_1, \psi_2\}$
- Hamiltonian is given by $H_{11} = \langle \psi_1 | \hat{H} | \psi_1 \rangle$, H_{22} , $H_{12} = H_{21}$
- Diagonalizing: $E_{1,2} = \frac{H_{11} + H_{22}}{2} \pm \frac{1}{2} \sqrt{(H_{11} - H_{22})^2 + 4H_{12}^2}$

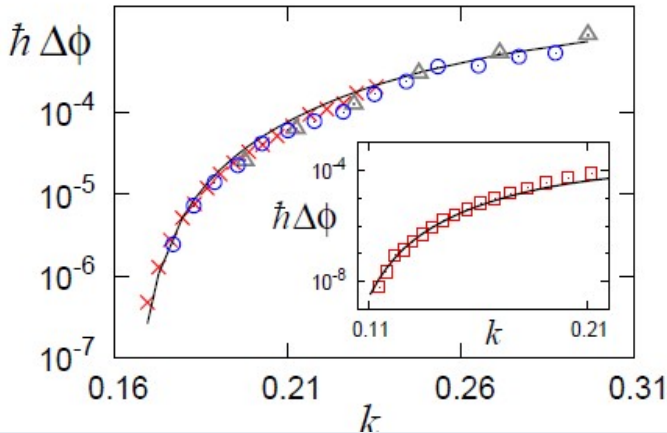


One avoided crossing



$$\Delta n = 6 \text{ with } n_{low} = 4 \text{ and } n_{up} = 10$$

Semiclassical analysis of $\Delta\phi$

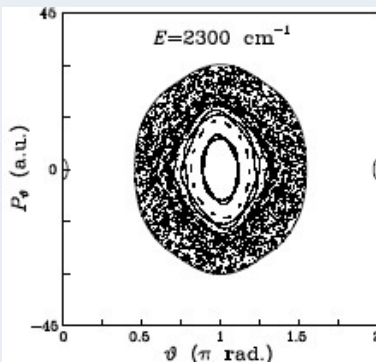


$\Delta n = 6$: $N=30$ (\triangle), 60 (\circ), and 100 (\times)



Thanks for your attention

Same thing with LiCN



Same thing with LiCN

